AJRCMB Articles in Press. Published on 26-January-2018 as 10.1165/rcmb.2017-0223OC

Upregulation and nuclear location of MMP28 in alveolar epithelium of Idiopathic Pulmonary Fibrosis

Running title: MMP28 in IPF

Mariel Maldonado[1], Alfonso Salgado-Aguayo[2], Iliana Herrera[2], Sandra Cabrera[1], Blanca Ortíz-Quintero[2], Claudia A. Staab-Weijnitz[3], Oliver Eickelberg[3,4], Remedios Ramírez[1], Anne M. Manicone[5], Moisés Selman[2], Annie Pardo[1].

1. Facultad de Ciencias, Universidad Nacional Autónoma de México, Mexico city, Mexico.
2. Instituto Nacional de Enfermedades Respiratorias Ismael Cosío Villegas, Mexico city, Mexico.
3. Comprehensive Pneumology Center, Helmholtz Zentrum München, Member of the German Center of Lung Research (DZL), Munich, Germany.
4. Division of Pulmonary and Critical Care Medicine, School of Medicine, University of Colorado, Denver, United States.
5. Department of Medicine, Center for Lung Biology, University of Washington, Seattle, Washington, United States.

Correspondence
Annie Pardo PhD
Facultad de Ciencias, Universidad Nacional Autónoma de México
Ciudad de Mexico, Mexico
Telephone: (52 55) 56233822
E-mail: apardos@unam.mx

Mariel Maldonado is a doctoral student from Programa de Doctorado en Ciencias Biomédicas, Universidad Nacional Autónoma de México (UNAM) and received the fellowship 275771 from Consejo Nacional de Ciencia y Tecnología, México (CONACyT).

Sources of support: This research was partially supported by UNAM PAPIIT: IN218516 and CONACYT 251636.

Author contributions:

M.M., A.P., conceived and designed the study. M.M. performed the bulk of the experiments. A.S.-A., I.H., B.O.-Q., R.R., assisted data acquisition. **C.A.S.-W., O.E.** provided IPF lung samples and human primary basal bronchial epithelial cells. S.C. conducted the experiments involving mice. M.M., A.S.-A., I.H., B.O.-Q., **C.A.S.-W., O.E., A.M.M,** M.S, A.P. participated in analysis of data. M.M., M.S., A.P. interpreted and discussed the data and wrote the manuscript. All authors revised the manuscript.

AJRCMB Articles in Press. Published on 26-January-2018 as 10.1165/rcmb.2017-0223OC

ABSTRACT

Idiopathic Pulmonary Fibrosis (IPF) is a chronic and progressive aging-associated disease of unknown etiology. Growing body of evidence indicates that aberrant activated alveolar epithelial cells induce the expansion and activation of the fibroblast population leading to the destruction of the lung architecture. Some Matrix Metalloproteinases (MMPs) are upregulated in IPF, indicating that they may be important in the pathogenesis and/or progression of IPF. Here, we studied the expression of MMP28 in this disease and evaluated its functional effects in two alveolar epithelial cell lines and in human primary bronchial epithelial cells. We found that the enzyme is expressed in bronchial (apical and cytoplasmic localization) and alveolar epithelial cells (cytoplasmic and nuclear localization) in two different IPF groups of patients. *In vitro*, MMP28 epithelial silencing decreased the proliferation rate and delayed wound closing, while overexpression showed the opposite effects, protected from apoptosis and enhanced epithelial-mesenchymal transition (EMT). Our findings demonstrate that MMP28 is upregulated in epithelial cells from IPF lungs where it may play a role in increasing the proliferative and migratory phenotype in a catalytic-dependent manner.

Key words: MMP, lung epithelial cells, IPF

Abbreviations: Alveolar Epithelial Cells (AEC), Bronchial Epithelial Cells (Airway epithelial cells: BEC), Epithelial-Mesenchymal Transition (EMT), Immunohistochemistry (IHC), Immunofluorescence (IF), Idiopathic Pulmonary Fibrosis (IPF), keratin 5 (krt5), Matrix Metalloproteinase-28 (MMP28), wildtype (WT).

INTRODUCTION

Idiopathic Pulmonary Fibrosis (IPF) is a progressive and aging related fibrosing interstitial pneumonia of unknown etiology (1-4). IPF is a complex epithelial-driven disorder where genetic, epigenetic and environmental factors interact triggering the aberrant activation of lung epithelium. In turn, hyperactivated alveolar epithelial cells produce numerous mediators that result in an increase of the fibroblast/myofibroblast population, excessive accumulation of extracellular matrix (ECM) and the destruction of lung architecture (1, 2, 5, 6).

From the complex pathways likely involved in the pathogenesis of IPF, deregulation in the expression of numerous Matrix Metalloproteinases (MMPs) has been consistently reported suggesting that they may be important in the pathogenesis and/or progression of IPF (7). MMPs are a family of zinc-dependent endopeptidases with 23 members in the human. These enzymes not only cleave ECM components, but also cytokines, growth factors, receptors and other bioactive molecules participating in cellular processes such as differentiation, proliferation and angiogenesis (8).

In 2001, the last member of the human MMP family was discovered simultaneously by two research groups (9, 10). MMP28 (epilysin) is expressed during development and regeneration of nervous system before myelination and in this circumstances, three substrates, still the only ones described for MMP28 so far, have been suggested: neural cell adhesion molecule (NCAM), nogo A and neuregulin (11). MMP28 mRNA has been found in many human epithelia, thus a role in homeostasis has been suggested (9). MMP28 has also been revealed in some pathological conditions including osteoarthritis and gastric carcinoma (12, 13). In murine lung, it has been demonstrated that MMP28 is expressed by Club cells (14) promoting epithelial cell survival *in vitro* and in a model of influenza infection (15). Loss of Mmp28 in mice results in reduced macrophage polarization to M2 phenotype and attenuation of bleomycin-induced lung fibrosis (16). More recently, it was found that Mmp28 deficient mice are also protected from tobacco-smoke induced inflammation and emphysema suggesting a role in chronic obstructive pulmonary disease (COPD) (17).

AJRCMB Articles in Press. Published on 26-January-2018 as 10.1165/rcmb.2017-0223OC

However, this enzyme has not been studied in human fibrotic lung disorders. In this context, the aim of this study was to evaluate the expression and localization of MMP28 in IPF, and analyze its functional effects in alveolar and airway epithelial cells *in vitro*.

MATERIALS and METHODS

Human samples

The human samples were obtained under protocols approved by the local ethics committees and all participants gave written informed consent. Samples from ~~the~~ 17 Mexican ~~cohort~~ patients were obtained at Instituto Nacional de Enfermedades Respiratorias (INER). Samples from ~~the~~ 9 German ~~cohort~~ patients were kindly provided by the CPC-M BioArchive at the Comprehensive Pneumology Center. Some demographic characteristics of the patients are included in table E1. Four liquid nitrogen-frozen tissues from IPF patients and four from donors, were homogenized using a microdismembrator (Sartorius) and lysed with RIPA buffer for protein isolation and western blot analysis, as described previously (18).

Cell culture

Human alveolar epithelial cell line A549 (AEC) and rat alveolar epithelial cell line RLE-6TN (rat AEC) were purchased from the American Type Culture Collection (ATCC). Human primary alveolar epithelial cells type II (19) (kindly donated by Melanie Königshoff) and human primary basal bronchial epithelial cells (BEC) had been isolated from a histologically normal tumor-free region of a lung tumor resection and were provided by the CPC-M BioArchive at the Comprehensive Pneumology Center. All cells were cultured in an incubator (5% CO2- 95% air) at 37°C. Cells were lysed with RIPA buffer, or cytoplasmic and nuclear enriched fractions were obtained with the NE-PER kit (78835, Thermo Scientific).

Silencing and overexpression

Silencing of MMP28 in AEC was performed using lentiviral particles (Santa Cruz) with scrambled control shRNA (sc-108080) or shMMP28 (sc-62278-V). For silencing of MMP28 in BEC, reverse transfection was achieved with scrambled siRNA (AM4611,

Ambion) or siMMP28 (s35627, Ambion). For overexpression, AEC and rat AEC were transfected with empty vector pCMV6-Entry (Mock, PS100001, Origene), fusion MMP28-DDK (MMP28, RC215325, Origene), catalytically inactive MMP28-DDK (EA) or KQ mutated MMP28-DDK (KQ).

For **imaging** and **western blot**, see supplementary methods.

Functional Effects

Functional effects were evaluated according to the supplier's recommendations for each test. *Growth rate* was studied with the WST-1 reagent (Roche). *Proliferation rate* was measured with the CyQUANT reagent (Thermo Fischer Scientific). Early a*poptosis* was determined with Annexin V by flow cytometry through the externalization of phosphatidylserine. *Wound assay* was performed as previously reported (20). *Transmigration* was evaluated with Collagen I coated 8μm transwells using 50ng/mL of EGF as chemoattractant (QCM Haptotaxis Cell Migration Assay – Collagen1, Colorimetric ECM582 Millipore). See supplementary methods for details.

Murine pulmonary fibrosis model

C57BL/6 wild type and Mmp28 deficient mice were kindly provided by Anne Manicone. The generation of the mice is described in (14). The mice were housed in specific pathogen-free conditions. All experiments were approved by the Ethics Committee at INER. Pulmonary fibrosis was induced by a single intratracheal instillation of 10mg of bleomycin sulfate (Cayman chemical) in 50uL of saline solution. Control groups received only the vehicle. Mice were sacrificed at 14 days after instillation. Left lungs were frozen and consigned for hydroxyproline determination. Right lungs were fixed with 4% paraformaldehyde for immunohistochemistry and staining with hematoxylin-eosin and Masson's trichrome.

Statistics

All experiments were performed three times by triplicate, unless stated otherwise. Results are given as mean ±SD, if not mentioned otherwise. ANOVA with Tukey or Dunnett's

AJRCMB Articles in Press. Published on 26-January-2018 as 10.1165/rcmb.2017-0223OC

adjustment for multiple comparisons was applied. $P<0.05$ was considered significant. Results were analyzed with GraphPad Prism version 5.

RESULTS

MMP28 is upregulated in IPF lungs and expressed by epithelial cells

Dataset from previous research suggested that MMP28 gene expression was increased in IPF lungs compared to controls (21). To validate this finding at the gene and protein level, lung tissue samples from IPF (n=7) and control donors (n=6) were analyzed by qRT-PCR and western blot. As illustrated in **Figure 1**, MMP28 showing bands of ~58 (proenzyme), ~48 and 46 kDa representatives of the molecular weight of the active enzyme was significantly increased in IPF ($p<0.01$). No significant differences were found by qRT-PCR (not shown).

Cellular localization of MMP28 in IPF and control lungs was examined by IHC and IF. MMP28 was mostly expressed by alveolar epithelial cells (AEC) in IPF, **(Figure 2 B, D, J, L)** and it was weakly expressed by the normal alveolar epithelium **(Figure 2 A, C, I, K).**
In addition to a cytoplasmic localization, a notable nuclear staining was found in AEC **(Figure 2 D, L)**. MMP28 was also observed in airway epithelial cells, **(Figure 2 F, N, P)**, which were identified by CC10 expression. Here, the staining was mainly apical and sometimes cytoplasmic.
To confirm the nuclear location of MMP28 in AEC, Z-stacks were obtained with confocal microscopy which demonstrated that the staining of MMP28 was inside the nucleus in some cells of IPF lungs **(Figure E1 A, B)** while in others it was perinuclear **(Figure E1C).** MMP28 was also observed to be coexpressed with keratin 5 (krt5) in some areas **(Figure 2 J, L)**. Although krt5 has been mainly described in progenitor airway epithelial cells (22), recent single-cell research performed in IPF lungs has demonstrated that alveolar epithelial cells show an aberrant phenotype, displaying both airway and alveolar proteins (23). As shown in **Figure E1E**, A549 alveolar epithelial cells also express krt5. To further corroborate the nuclear expression by alveolar epithelial cells in vivo, IPF lungs were costained with SP-C and MMP-28 and examined by immunofluorescence **(Figure 2 S)**.

Intracellular localization of MMP28 in alveolar and bronchial epithelial cells *in vitro*

AJRCMB Articles in Press. Published on 26-January-2018 as 10.1165/rcmb.2017-0223OC

To evaluate whether MMP28 is present in the nucleus of lung epithelial cells *in vitro*, we performed IF of fixed A549, and primary alveolar and bronchial epithelial cells (BEC). In the case of the A549 cell line, many of them showed cytoplasmic signal, but in some cells a clear nuclear localization was observed **(Figure 3 A, B)**, which was confirmed by the z-stacks (**Figure 3 C**). Nuclear localization was also observed in some primary human AEC (**Figure 3 D**). In primary human differentiated bronchial epithelial cells MMP28 was only detected in the cytoplasm, colocalizing with the endoplasmic reticulum protein ERp57 (**Figure 3 E, F**). This finding correlates with our observations *in vivo* (IHC and IF).

To verify the intracellular MMP28 localization in AEC, nuclear and cytoplasmic fractions of A549 native cells were obtained. As shown in **Figure 3 G** the presence of the enzyme in the nuclear fraction was confirmed. A ~48-50 kDa band likely representing the active form of the enzyme was revealed in the nuclear compartment, while in the cytoplasmic portion a ~60-62kDa band, probably representing the proform, was observed.

Looking for a possible MMP28 nuclear translocation mechanism we performed an *in silico* analysis using two different software tools (see supplementary methods). Both revealed the same likely nuclear localization signal (NLS): 112-RHRTKMRRKKR-122 (Prediction cutoff 0.7). To find out whether the mechanism to enter the nucleus depends on this putative NLS, we performed site-directed mutagenesis to change lysines to glutamines in the NLS (K116Q, K120Q and K121Q, polar amino acids with similar molecular weight and no charge). A549 cells were transfected either with DDK-tagged MMP28 (WT-MMP28), or with DDK-tagged MMP28 mutant (KQ-MMP28) or empty vector (Mock, PS100001 Origene).

Cells were analyzed by imaging flow cytometry with an anti-DDK antibody. **Figure E2A** shows that ~24% of the cells transfected with the KQ-MMP28 present a nuclear location of the protein with no significant differences with the WT-MMP28 transfected cells (~ 29%). Likewise, analyzing Mock, WT-MMP28 and KQ-MMP28 cells with anti-MMP28, which binds to the transfected protein as well as to the endogenous protein, we found that around 30% of Mock cells lacking transfected protein showed a nuclear location of MMP-28 that increased to 45% in the transfected cells. **Figure E2B** illustrates a representative image of Mock, WT-MMP28 and KQ-MMP28 cells with nuclear or cytoplasmic localization of the enzyme.

Effects of overexpression and silencing of MMP28 *in vitro*

In order to analyze the possible role of MMP28 in AEC and BEC, human A549 cell line, rat RLE-6TN alveolar epithelial cell line (rat AEC), and primary human BEC were used. AEC (A549 and RLE-6TN) were transfected with human WT MMP28 DDK tag (*MMP28*) **(Figure E3 A, B, E, F)**. While intracellular MMP28 levels were moderately increased, extracellular MMP28 was drastically increased. Additionally, MMP28 was silenced in A549 cells using shRNA (*shMMP28)* achieving 80% of efficiency at RNA level and 70% at protein level in one of the clones **(Figure E3 C, D)**. Also, MMP28 expression in primary human BEC was transiently decreased with siRNA (*siMMP28)* getting around 70% of knockdown efficiency from 24 to 72 hours of culture **(Figure E3 G, H)**.

MMP28 increases proliferation and growth rate ~~and protects from apoptosis~~

Overexpression of MMP28 in AEC significantly increased their growth and proliferation rates compared with their controls ($p < 0.001$). By contrast, when MMP28 was silenced, growth and proliferation rates significantly decreased ($p<0.001$) **(Figure 4 A, B).** Similarly, the transfection of human MMP28 to rat AEC significantly increased their growth and proliferation rates compared with Mock ($p<0.001$) **(Figure E4 A, B)**. Regarding primary human BEC, when MMP28 was silenced a significant decrease in growth and proliferation rates was also observed ($p<0.001$) **(Figure E4 C, D).**

We examined whether nuclear MMP-28 colocalized with the proliferation biomarker phospho-Histone H3 (Ser10, pH3). As illustrated in **figure 4C and D**, some IPF epithelial cells showed nuclear colocalization of MMP-28 and pH3.

MMP28 protects epithelial cells from apoptosis, promotes migration and enhances epithelial to mesenchymal transition.

Given that the growth rate includes cell proliferation and cell death, the effect of MMP28 on apoptosis was also evaluated using bleomycin as an apoptotic stimulus. As shown in **Figure 5 A**, MMP28 overexpression significantly protected AEC from apoptosis ($p < 0.05$), while silencing the enzyme induced an increase in apoptosis ($p < 0.01$).

AJRCMB Articles in Press. Published on 26-January-2018 as 10.1165/rcmb.2017-0223OC

Cell migration was evaluated by the scratch wound healing assay. As shown in **Figure 5B**, at 48h, in A549 cells transfected with MMP28 the wound closed 94.5±4% while healing was only 70.7±3% using Mock cells. By contrast, MMP28 silenced cells delayed this process with 52±6.8% of wound extension at 48h. There was no significant difference between Mock and shCtrl cells. Likewise, overexpression of MMP28 in rat AEC accelerated wound closing 88.56±3.6% versus 55.15±14.46% in Mock cells at 12h **(Figure E5 A)**, while silencing of MMP28 in BEC delayed wound closing at 18h to 40±16% versus 74.7±6.5% obtained with the scrambled RNA treated cells **(Figure E5 B).**

Transmigration of AEC performed in Boyden chambers covered with collagen I revealed that overexpression of MMP28 increased transmigration in 42±4% ($p<0.001$), while silencing of MMP28 decreased it in 26±10.7% ($p<0.01$) **(Figure 5C).**

There have been contradictory results regarding a putative role of MMP28 on epithelial-mesenchymal transition (EMT) (15, 24). We tested this effect on A549 epithelial cells. We observed that the expression of E-cadherin (as an epithelial marker) in MMP28 transfected cells was remarkably decreased compared with Mock transfected cells under basal conditions, and when stimulated with TGFβ1 for two days this effect was amplified (**Figure 5D**). The presence of fibronectin as a mesenchymal marker was observed until the fourth day of TGFβ1 stimulation, and with the overexpression of MMP28 the intensity of the fibronectin band increased (**Figure 5E**).

Effects of MMP-28 on migration and proliferation are catalytic-dependent

In order to test if the functional effects observed were due to the catalytic activity of MMP28, site-directed mutagenesis was performed based on previous reports (15, 24) to change the glutamate in the catalytic site for an alanine (E241A, see Methods). Human AEC and rat AEC were transfected with the EA mutant MMP28 and the experiments evaluating functional effects were repeated. As shown in **Figure 6A-D**, the increase in growth rate and the accelerated wound closure observed in cells transfected with WT MMP28 are not preserved in cells transfected with the EA mutant MMP28. Consequently, these are catalytic-dependent effects of MMP28.

Analysis of Mmp28 in the murine model of pulmonary fibrosis

As reported before (14), in healthy mice lungs Mmp28 is expressed by airway epithelial cells, but also by some AEC. At 14 days after bleomycin injury, immunoreactive Mmp28 expression was observed in addition to epithelium in intra-alveolar macrophages ((Figure 7A). After 14 days of bleomycin instillation, we observed a significant increase of Mmp28 at the protein level (Figure 7B).

It has been previously reported that *Mmp*28-deficient mice showed a modest reduction of collagen accumulation at days 14 and 21 after low dose of bleomycin injury (16). With the usual dose that we utilize, we corroborated that *Mmp*28 -/- mice develop less fibrosis at day 14 of the fibrotic phase of the model. In panel 7C representative images of Masson's trichrome are shown and a significantly lower hydroxyproline content in lungs of *Mmp*28-deficient mice was observed (Figure 7D).

To confirm our results with epithelial cell lines, we isolated primary lung epithelial cells from WT and *Mmp*28 -/- mice and performed transmigration assays in Boyden chambers covered with collagen I. As shown in Figure 7E we revealed that cells from *Mmp*28-deficient mice showed significant less migration compared with WT mice.

AJRCMB Articles in Press. Published on 26-January-2018 as 10.1165/rcmb.2017-0223OC

DISCUSSION

IPF is a complex disorder where the interaction of aging and multiple genetic and environmental risk factors results in the hyperactivation of the alveolar epithelium that triggers an aberrant wound healing response to repetitive lung micro-injuries. In this pathological process, a variety of mediators such as growth factors, cytokines, chemokines and coagulation factor receptors are involved (1, 2). In this context, a growing body of evidence supports a critical role of MMPs either releasing or activating growth factors such as TGFβ, or actively participating in lung remodeling processes. Most of them are expressed by the aberrantly activated alveolar epithelium, and may play profibrotic (e.g. MMP-7), or antifibrotic roles (e.g., MMP-19) (25, 26).

In this study, we focused on MMP28, the last revealed member of the MMP family. This enzyme has the typical structural domains of the MMPs consisting of a signal peptide at the N-terminus that leads it through the secretory pathway, a prodomain that keeps it as zymogen, a catalytic domain with a Zinc ion, and a hinge region that is adjacent to the four hemopexin-like domains in the C-terminus. Between the prodomain and the catalytic domain it has the RKKR motif classically recognized by proprotein convertases; however, MMP28 is not identified by furin at this site but at an upstream YGYL motif (specifically at the Y45L46) in the prodomain (27).

In the present study we examined the expression, localization and possible functions of MMP28 in IPF, a usually progressive and irreversible epithelial-driven fibrosis. We found that the enzyme is mainly expressed by the lung epithelium, specifically by alveolar and bronchial epithelial cells. Interestingly, immunohistochemical detection with four different antibodies revealed that, in some alveolar epithelial cells, MMP28 localized in the nuclei, a finding that was confirmed with z-stacks from human tissues and cultured cells. The enzyme was also observed in the nuclei of krt5+ (likely) progenitor cells that have been recently found in fibrotic areas of IPF lungs (22), and in the nuclei of proSP-C positive cells, a biomarker of alveolar epithelial cells type II. By contrast, in BEC, MMP28 staining was mostly apical. It is important to emphasize that in IPF, many lung epithelial cells acquire aberrant, multilineage-like states and some of them share characteristics of both

conducting airway and alveolar epithelial cells (23). Moreover, the A549 cell line that was used in this study also expressed krt5.

Notably, while Mexican IPF biopsies were obtained from patients at the time of diagnosis, German IPF samples were explants obtained during lung transplantation, thus representing end-stage disease, indicating that the epithelial expression of this enzyme is maintained during the progression of the disease.

The roles of MMPs have mostly been described in the extracellular environment; however, some of them have been previously found in intracellular compartments, such as nuclei and mitochondria (20, 28-34). Specifically, nuclear localization has been shown for MMP2, MMP3, MMP12 and MMP14, where these proteins have been proposed to have certain roles as transcriptional (co)factors or as apoptosis-related proteases (35-41). Nevertheless, a nuclear localization of MMP28 has not been reported before.

There are some studies showing that nuclear translocation of MMPs may be dependent of new NLSs found in their sequences (35, 36, 40). In the case of MMP28, a putative NLS was found between the prodomain and the catalytic domain. Nevertheless, changing the lysines for glutamines in the putative NLS did not modify the localization of the enzyme suggesting that this sequence is not a real NLS, thus MMP28 nuclear translocation deserves further studies.

The putative role of epithelial expression of MMP28 in IPF is presently unclear. By gain-and-loss experiments, we found that the enzyme increases epithelial growth rate, proliferation and migration. Interestingly, we found that in IPF lungs epithelial nuclear MMP28 colocalizes with the marker of proliferation phospho histone H3 suggesting that it might be related to a proliferative phenotype, one of the features described in a subset of IPF epithelial cells. Additionally, we confirmed that MMP28 confers resistance to apoptosis as previously reported (15).

These functions were lost when the catalytic domain was affected by site-directed mutagenesis changing the glutamate in the catalytic site for an alanine. This finding supports the hypothesis that the catalytic activity of MMP28 promotes an invasive phenotype in AEC as suggested previously (24). In fact, in gastric carcinoma and in several gastric cancer cell lines, MMP28 is increased and correlates with a greater invasive

AJRCMB Articles in Press. Published on 26-January-2018 as 10.1165/rcmb.2017-0223OC

phenotype (13). Regarding the role of MMP28 in EMT, contradictory results have been documented (15, 24). Our results indicate that this enzyme enhanced this process and interestingly we found that while the epithelial marker E-cadherin was modified earlier, the mesenchymal marker fibronectin appeared only after four days of TGF-β stimulation in the MMP28 transfected cells.

The finding that the increase in proliferation and wound closure was observed not only in AEC, but also in BEC suggest that these effects are not only related with the nuclear MMP28. Future approaches are necessary to identify protein binding partners and/or target DNA sequences, and should include high throughput proteomics in order to analyze substrates as well as the signaling pathways of the effects we have described.

Taking together, our findings indicate that MMP28 is expressed in the IPF lungs mainly by epithelial cells enhancing survival, proliferation/migration and EMT. Some of these processes characterize the aberrantly activated epithelial cells in IPF. However, the pathological result of these effects in vivo is presently unclear.

MMP28 has been described as profibrotic in the bleomycin-induced lung injury model (16), Recently, MMP28 has also been implicated in the pathogenesis of tobacco-smoke induced emphysema (17). In both experimental murine models, Mmp28 was expressed primarily by lung macrophages. We found that Mmp28 is also expressed by alveolar epithelial cells and corroborated the profibrotic role in the model. Moreover, we found that Mmp 28 -/- lung epithelial cells displayed a less migratory phenotype versus WT cells.

In conclusion, our study demonstrated the up-regulation of MMP28 in IPF lungs where it is expressed in bronchial (*apical and cytoplasmic localization*) and alveolar epithelial cells (*cytoplasmic and nuclear localization*) in two different IPF groups of patients ~~cohorts~~. *In vitro* MMP28 protects lung epithelial cells from apoptosis, increases proliferation and migration, and enhances EMT in a catalytic-dependent manner.

Acknowledgments

Jorge García-Alvarez, Fien M. Verhamme, Mariana Maciel, Miguel Gaxiola.

References

1. King TE Jr, Pardo A, Selman M. Idiopathic pulmonary fibrosis. *Lancet.* 2011;378:1949-61.

2. Selman M, Pardo A. Revealing the pathogenic and aging-related mechanisms of the enigmatic idiopathic pulmonary fibrosis. An integral model. *Am J Respir Crit Care Med.* 2014;189:1161-72.

3. Raghu G, Collard HR, Egan JJ, Martinez FJ, Behr J, Brown KK, Colby TV, Cordier JF, Flaherty KR, Lasky JA, Lynch DA, Ryu JH, Swigris JJ, Wells AU, Ancochea J, Bouros D, Carvalho C, Costabel U, Ebina M, Hansell DM, Johkoh T, Kim DS, King TE Jr, Kondoh Y, Myers J, Müller NL, Nicholson AG, Richeldi L, Selman M, Dudden RF, Griss BS, Protzko SL, Schünemann HJ; ATS/ERS/JRS/ALAT. Committee on Idiopathic Pulmonary Fibrosis. An official ATS/ERS/JRS/ALAT statement: idiopathic pulmonary fibrosis: evidence-based guidelines for diagnosis and management. *Am J Respir Crit Care Med.* 2011;183:788-824.

4. Thannickal VJ, Murthy M, Balch WE, Chandel NS, Meiners S, Eickelberg O, Selman M, Pardo A, White ES, Levy BD, Busse PJ, Tuder RM, Antony VB, Sznajder JI, Budinger GR. Blue journal conference. Aging and susceptibility to lung disease. *Am J Respir Crit Care Med.* 2015;191:261-9.

5. Selman M, King Jr TE, Pardo A. Idiopathic Pulmonary Fibrosis: Prevailing and Evolving Hypotheses about Its Pathologenesis and Implications for Therapy. *Ann Intern Med.* 2001;134:136-151.

6. Selman M, López-Otín C, Pardo A. Age-driven developmental drift in the pathogenesis of idiopathic pulmonary fibrosis. *Eur Respir J.* 2016;48(2):538-52.

AJRCMB Articles in Press. Published on 26-January-2018 as 10.1165/rcmb.2017-0223OC

7. Pardo A, Cabrera S, Maldonado M, Selman M. Role of matrix metalloproteinases in the pathogenesis of idiopathic pulmonary fibrosis. *Respir Res*. 2016;17:23. doi: 10.1186/s12931-016-0343-6.

8. Bonnans C, Chou J, Werb Z. Remodelling the extracellular matrix in development and disease. *Nat Rev Mol Cell Biol.* 2014;15:786-801.

9. Lohi J, Wilson CL, Roby JD, Parks WC. Epilysin, a Novel Human Matrix Metalloproteinase (MMP-28) expressed in Testis and Keratinocytes and in Response to Injury. *J Biol Chem.* 2001;276(13): 10134–10144.

10. Marchenko GN, Strongin AY. MMP-28, a new human matrix metalloproteinase with an unusual cysteine-switch sequence is widely expressed in tumors. *Gene* 2001;265:87-93.

11. Werner SR, Mescher AL, Neff AW, King MW, Chaturvedi S, Duffin KL, Harty MW, Smith RC. Neural MMP-28 Expression Precedes Myelination During Development and Peripheral Nerve Repair. *Developmental Dynamics* 2007;236:2852–2864.

12. Momohara S, Okamoto H, Komiya K, Ikari K. Matrix metalloproteinase 28/epilysin expression in cartilage from patients with rheumatoid arthritis and osteoarthritis: comment on the article by Kevorkian et al. *Arthritis Rheum.* 2004;50(12): 4074–5; author reply 4075.

13. Jian P, Yanfang T, Zhuan Z, Jian W, Xueming Z, Jian N. MMP28 (epilysin) as a novel promoter of invasion and metastasis in gastric cancer. *BMC Cancer*. 2011;11:200.

14. Manicone AM, Birkland TP, Lin M, Betsuyaku T, van Rooijen N, Lohi J, Keski-Oja J, Wang Y, Skerrett SJ, Parks WC. Epilysin (mmp-28) restrains early macrophage recruitment in pseudomonas aeruginosa pneumonia. *J Immunol*. 2009;182:3866-3876.

15. Manicone AM, Harju-Baker S, Johnston LK, Chen AJ, Parks WC. Epilysin (matrix metalloproteinase-28) contributes to airway epithelial cell survival. *Respir Res.* 2011;12:144.

16. Gharib SA, Johnston LK, Huizar I, Birkland TP, Hanson J, Wang Y, Parks WC, Manicone AM. MMP28 promotes macrophage polarization toward M2 cells and augments pulmonary fibrosis. *J Leukoc Biol.* 2014;95:9-18.

17. Manicone AM, Gharib SA, Gong KQ, Eddy WE, Long ME, Frevert CW, Altemeier WA, Parks WC, Houghton AM. Matrix Metalloproteinase-28 Is a Key Contributor to Emphysema Pathogenesis. *Am J Pathol.* 2017;187(6):1288-1300.

18. Staab-Weijnitz CA, Fernandez IE, Knüppel L, Maul J, Heinzelmann K, Juan-Guardela BM, Hennen E, Preissler G, Winter H, Neurohr C, Hatz R, Lindner M, Behr J, Kaminski N, Eickelberg O. FK506-Binding Protein 10, a Potential Novel Drug Target for Idiopathic Pulmonary Fibrosis. *Am J Respir Crit Care Med* 2015;192(4):455-467.

19. Königshoff M, Kramer M, Balsara N, Wilhelm J, Amarie OV, Jahn A, Rose F, Fink L, Seeger W, Schaefer L, Günther A, Eickelberg O. WNT1-inducible signaling protein-1 mediates pulmonary fibrosis in mice and is upregulated in humans with idiopathic pulmonary fibrosis. J Clin Invest. 2009;119(4):772-87.

20. Herrera I, Cisneros J, Maldonado M, Ramírez R, Ortiz-Quintero B, Anso E, Chandel NS, Selman M, Pardo A. Matrix metalloproteinase (MMP)-1 induces lung alveolar epithelial cell migration and proliferation, protects from apoptosis, and represses mitochondrial oxygen consumption. *J Biol Chem.* 2013;288:25964-25975.

21. Pardo A, Selman M, Kaminski N. Approaching the degradome in idiopathic pulmonary fibrosis. *Int. J. Biochem. Cell Biol.* 2008;40:1141–1155.

AJRCMB Articles in Press. Published on 26-January-2018 as 10.1165/rcmb.2017-0223OC

22. Smirnova NF, Schamberger AC, Nayakanti S, Hatz R, Behr J, Eickelberg O. Detection and quantification of epithelial progenitor cell populations in human healthy and IPF lungs. *Respir Res.* 2016;17:83.

23. Xu Y, Mizuno T, Sridharan A, Du Y, Guo M, Tang J, Wikenheiser-Brokamp KA, Perl AT, Funari VA, Gokey JJ, Stripp BR, Whitsett JA. Single-cell RNA sequencing identifies diverse roles of epithelial cells in idiopathic pulmonary fibrosis. *JCI Insight.* 2016; 1(20): e90558.

24. Illman S, Lehti K, Keski-Oja J, Lohi J. Epilysin (MMP-28) induces TGF-beta mediated epithelial to mesenchymal transition in lung carcinoma cells. *J Cell Sci.* 2006;119:3856–3865.

25. Zuo F, Kaminski N, Eugui E, Allard J, Yakhini Z, Ben-Dor A, Lollini L, Morris D, Kim Y, DeLustro B, Sheppard D, Pardo A, Selman M, Heller RA. Gene expression analysis reveals matrilysin as a key regulator of pulmonary fibrosis in mice and humans. *Proc Natl Acad Sci* USA. 2002;99:6292–7.

26. Jara P, Calyeca J, Romero Y, Plácido L, Yu G, Kaminski N, Maldonado V, Cisneros J, Selman M, Pardo A. Matrix metalloproteinase (MMP)-19-deficient fibroblasts display a profibrotic phenotype. *Am J Physiol Lung Cell Mol Physiol.* 2015;308:L511-22.

27. Pavlaki M, Zucker S, Dufour A, Calabrese N, Bahou W, Cao J. Furin Functions as a Nonproteolytic Chaperone for MatrixMetalloproteinase-28: MMP-28 Propeptide Sequence Requirement. *Biochem Res Int.* 2011. Article ID 630319.

28. Limb GA, Matter K, Murphy G, Cambrey AD, Bishop PN, Morris GE, Khaw PT. Matrix metalloproteinase-1 associates with intracellular organelles and confers resistance to lamin A/C degradation during apoptosis. *Am J Pathol.* 2005;166:1555-63.

29. Ip YC, Cheung ST, Fan ST. Atypical localization of membrane type 1-matrix metalloproteinase in the nucleus is associated with aggressive features of hepatocellular carcinoma. *Mol Carcinog.* 2007;46, 225–230.

30. Choi DH, Kim EM, Son HJ, Joh TH, Kim YS, Kim D, Flint Beal M, Hwang O. A novel intracellular role of matrix metalloproteinase-3 during apoptosis of dopaminergic cells. *J Neurochem.* 2008;106(1):405-15.

31. Lovett DH, Mahimkar R, Raffai RL, Cape L, Maklashina E, Cecchini G, Karliner JS. A Novel Intracellular Isoform of Matrix Metalloproteinase-2 Induced by Oxidative Stress Activates Innate Immunity. *PLoS ONE.* 2012. 7(4): e34177.

32. Xiangyang Zuo, Wen Pan, Tingting Feng, Xiaohong Shi, Jianfeng Dai. Matrix Metalloproteinase 3 Promotes Cellular AntiDengue Virus Response via Interaction with Transcription Factor NFkB in Cell Nucleus. *PLoS One*. 2014;9(1):e84748.

33. DeCoux A, Lindsey ML, Villareal F, Garcia RA, Schulz R. Myocardial matrix metalloproteinase-2: inside out and upside down. *J Mol Cell Cardiol*. 2014;77:64-72.

34. Ceron CS, Baligand C, Joshi SK, Wanga S, Cowley PM, Walker JP, Song SH, Mahimkar R, Baker AJ, Raffai RL, Wang ZJ, Lovett DH. An intracellular matrix metalloproteinase-2 isoform induces tubular regulated necrosis: implications for acute kidney injury. *Am J Physiol Renal Physiol.* 2017;;312(6):F1166-F1183.

35. Eguchi T, Kubota S, Kawata K, Mukudai Y, Uehara J, Ohgawara T, Ibaragi S, Sasaki A, Kuboki T, Takigawa M. Novel transcription-factor-like function of human matrix metalloproteinase 3 regulating the CTGF/CCN2 gene. *Mol Cell Biol.* 2008;28:2391–2413.

36. Marchant DJ, Bellac CL, Moraes TJ, Wadsworth SJ, Dufour A, Butler GS, Bilawchuk LM, Hendry RG, Robertson AG, Cheung CT, Ng J, Ang L, Luo Z, Heilbron K, Norris MJ, Duan W, Bucyk T, Karpov A, Devel L, Georgiadis D, Hegele RG, Luo H, Granville DJ,

AJRCMB Articles in Press. Published on 26-January-2018 as 10.1165/rcmb.2017-0223OC

Dive V, McManus BM, Overall CM. A new transcriptional role for matrix metalloproteinase-12 in antiviral immunity. *Nature Med.* 2014;20:493-502.

37. Shimizu-Hirota R, Xiong W, Baxter BT, Kunkel SL, Maillard I, Chen XW, Sabeh F, Liu R, Li XY, Weiss SJ. MT1-MMP regulates the PI3Kδ•Mi-2/NuRD-dependent control of macrophage immune function. *Genes Dev.* 2012;26:395-413.

38. Eguchi T, Calderwood SK, Takigawa M, Kubota S, Kozaki KI. Intracellular MMP3 Promotes *HSP* Gene Expression in Collaboration With Chromobox Proteins. *J Cell Biochem.* 2017;118(1):43-51.

39. Kwan JA, Schulze CJ, Wang W, Leon H, Sariahmetoglu M, Sung M, Sawicka J, Sims DE, Sawicki G, Schulz R. Matrix metalloproteinase-2 (MMP-2) is present in the nucleus of cardiac myocytes and is capable of cleaving poly (ADP-ribose) polymerase (PARP) in vitro. *The FASEB Journal.* 2004;1, 690-692.

40. Si-Tayeb K, Monvoisin A, Mazzocco C, Lepreux S, Decossas M, Cubel G, Taras D, Blanc JF, Robinson DR, Rosenbaum J. Matrix metalloproteinase 3 is present in the cell nucleus and is involved in apoptosis. *Am J Pathol.* 2006;169(4):1390-1401.

41. Yang Y, Candelario-Jalil E, Thompson JF, Cuadrado E, Estrada EY, Rosell A, Montaner J, Rosenberg GA. Increased intranuclear matrix metalloproteinase activity in neurons interferes with oxidative DNA repair in focal cerebral ischemia. *J Neurochem.* 2010;112,134-149.

Figure Legends

Figure 1: ***MMP28 is increased in IPF.*** A. The expression of the MMP28 protein was analyzed by Western blot in 7 IPF and 6 control lungs from German (left) or Mexican (right) patients. B. Densitometric analysis represent 58, 48 and 46 kDa bands; ~~*p<0.05~~ **p<0.01.

Figure 2: ***MMP28 is expressed by alveolar and airway epithelial cells in IPF.*** Left panel: Immunohistochemical localization of MMP28 in control lungs (A, C, E) and in IPF (B, D, F). Right panel: MMP28 localization by immunofluorescence in control (I, K, M, O) and IPF lungs (J, L, N, P). For confocal microscopy, keratin 5 (krt5) was used as a marker of epithelial cells, CC10 as a marker of Club cells and DAPI for nuclei. IHC negative controls were incubated with no primary antibody (G, H). Rabbit IgG was used as negative control in IF (Q, R). S represents cells coexpressing prosurfactant protein C (pro SP-C) and MMP28 in merged with transmitted light differential interference contrast (DIC). IHC: IPF n=8, Ctrl n=5. IF: IPF n=5, Ctrl n=3.

Figure 3. ***MMP28 localization by immunofluorescence in epithelial cells in vitro.*** Native human alveolar epithelial cells (A549; A, B, C representing five independent experiments by triplicate), primary human AEC (D, two independent experiments), and primary human airway epithelial cells differentiated *in vitro,* (E, F, two independent experiments by duplicate). Cytoplasmic localization is indicated with white arrows, and nuclear localization with yellow arrows. XZ and YZ images from Z-stacks of AEC validate the nuclear localization of MMP28 (C). MMP28 colocalizes with ERp57 (F). G: Western blot of nuclear (N) and cytoplasmic (C) fractions from A549 cells. β-tubulin and lamin A/C were used as markers of cytoplasmic and nuclear fractions respectively. These are the results of two independent experiments by duplicate.

AJRCMB Articles in Press. Published on 26-January-2018 as 10.1165/rcmb.2017-0223OC

Figure 4. ***MMP28 induces proliferation in vitro and colocalizes with a proliferation biomarker in IPF lungs. protects from apoptosis and enhances epithelial to mesenchymal transition.*** MMP28 transfected or silenced A549 alveolar epithelial cells were evaluated for growth rate (A) and proliferation (B). Panels A and B show one representative experiment of four independent experiments by triplicate (data are presented as mean ±SD; ***p<0.001). Panel C show epithelial cells coexpressing anti-*phospho-Histone H3, a proliferation marker and MMP28.* n=2.

Figure 5. ***MMP28 protects from apoptosis, promotes migration and enhances epithelial to mesenchymal transition of A549 epithelial cells.***
Panel A illustrates the % of apoptosis induced by bleomycin. Results are expressed as mean ±SEM of three independent experiments (*p<0.05, **p<0.01). Panel B: Scratch assays with MMP28 transfected or silenced A549 cells. The magnification is 10x. The figure shows one representative experiment from four experiments performed by quadruplicate. Panel C: Transmigration over collagen I in Boyden chambers. One representative experiment of two independent experiments by triplicate. Panels D and E: Mock and MMP28 transfected cells were stimulated with TGF-β 1 for 2 days (D) and 4 days (E). E-cadherin was used as a marker of epithelial cells, and fibronectin as a marker of mesenchymal cells. Western blots are representative of three independent experiments.

Figure 6. ***MMP28 effects on migration and proliferation are catalytic-dependent.***
Cells were transfected with WT MMP28 (MMP28) or catalytically inactive MMP28 (EA), and proliferation (A and B) and wound closure (C and D) were measured. Each graph is representative of three experiments by triplicate. Data are presented as mean ±SD; *p<0.05, ***p<0.001).

Figure 7. ***Analysis of Mmp28 in murine pulmonary fibrosis model.*** WT mice after 14 days of saline or bleomycin instillation: Mmp28 IHC (A), Mmp28 western-blot (B). WT or Mmp28-deficient mice (KO) after 14 days of saline or bleomycin instillation: Masson's

trichrome (C), OH-Proline quantification (D), transmigration of lung epithelial enriched fraction over collagen I in Boyden chambers (E). Two independent experiments with n=6.

AJRCMB Articles in Press. Published on 26-January-2018 as 10.1165/rcmb.2017-0223OC

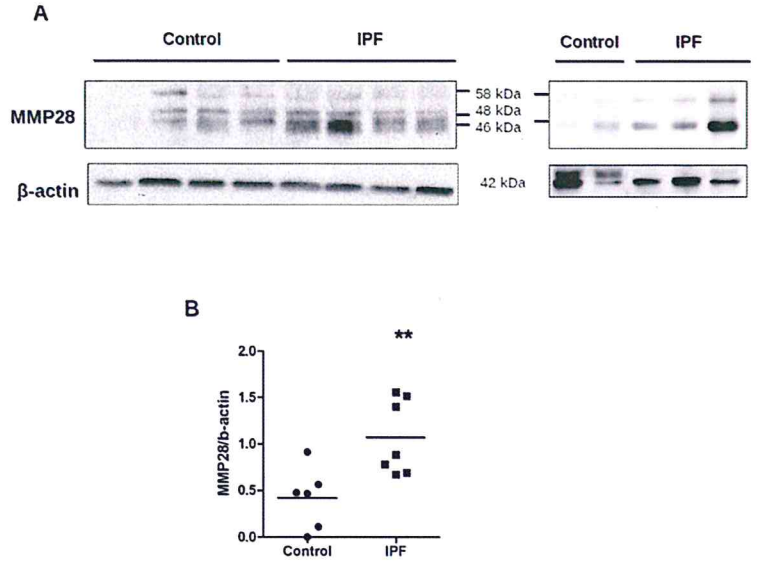

Figure 1

Figure 1. MMP28 is increased in IPF. A. The expression of the MMP28 protein was analyzed by Western blot in 7 IPF and 6 control lungs from German (left) or Mexican (right) patients. B. Densitometric analysis represent 58, 48 and 46 kDa bands; *p<0.05 **p<0.01.

55x44mm (600 x 600 DPI)

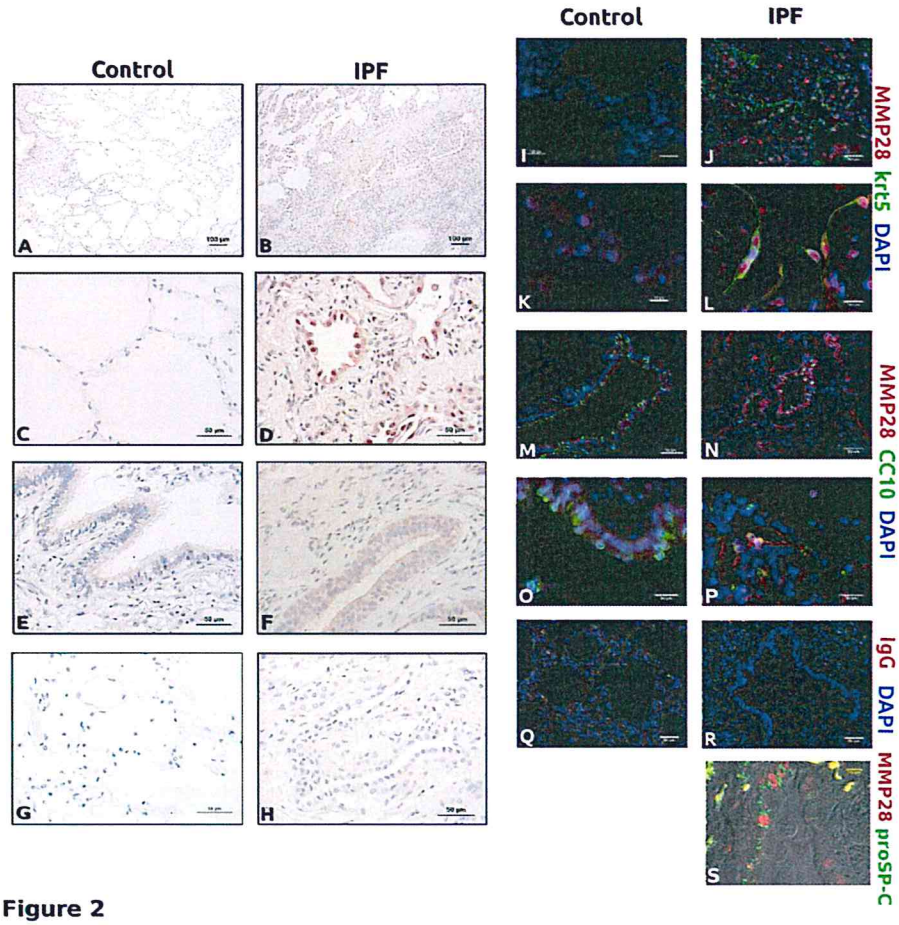

Figure 2

Figure 2. MMP28 is expressed by alveolar and airway epithelial cells in IPF. Left panel: Immunohistochemical localization of MMP28 in control lungs (A, C, E) and in IPF (B, D, F). Right panel: MMP28 localization by immunofluorescence in control (I, K, M, O) and IPF lungs (J, L, N, P). For confocal microscopy, keratin 5 (krt5) was used as a marker of epithelial cells, CC10 as a marker of Club cells and DAPI for nuclei. IHC negative controls were incubated with no primary antibody (G, H). Rabbit IgG was used as negative control in IF (Q, R). S represents cells coexpressing prosurfactant protein C (pro SP-C) and MMP28 in merged with transmitted light differential interference contrast (DIC). IHC: IPF n=8, Ctrl n=5. IF: IPF n=5, Ctrl n=3.

173x180mm (300 x 300 DPI)

AJRCMB Articles in Press. Published on 26-January-2018 as 10.1165/rcmb.2017-0223OC

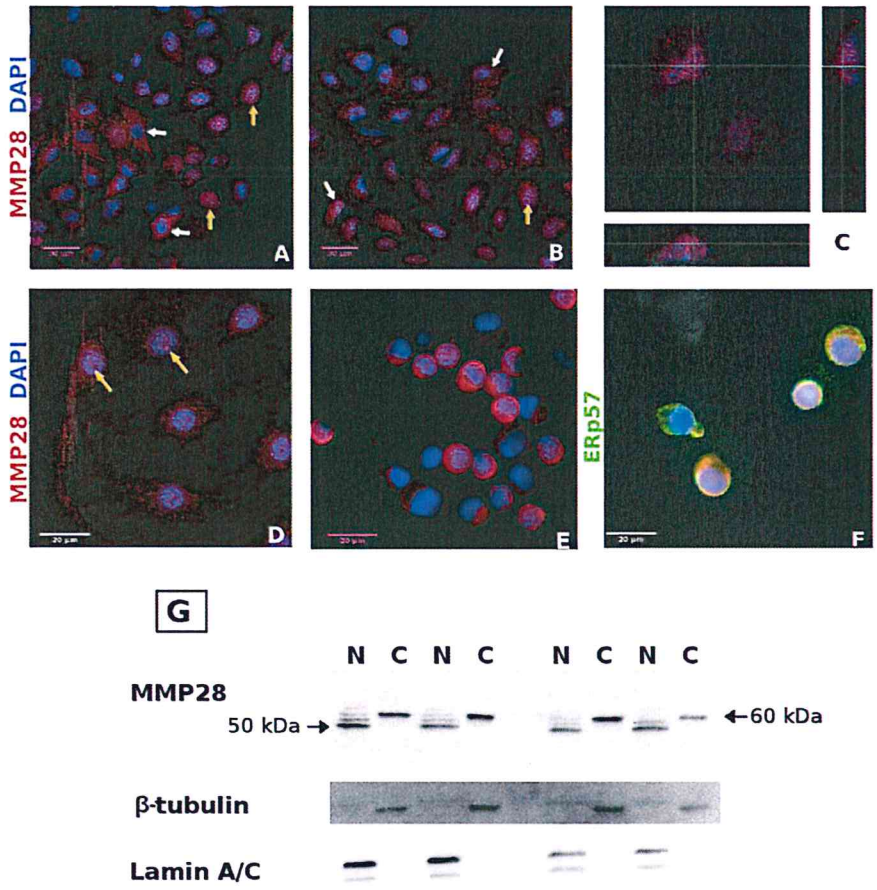

Figure 3

Figure 3. MMP28 localization by immunofluorescence in epithelial cells in vitro. Native human alveolar epithelial cells (A549; A, B, C representing five independent experiments by triplicate), primary human AEC (D, two independent experiments), and primary human airway epithelial cells differentiated in vitro, (E, F, two independent experiments by duplicate). Cytoplasmic localization is indicated with white arrows, and nuclear localization with yellow arrows. XZ and YZ images from Z-stacks of AEC validate the nuclear localization of MMP28 (C). MMP28 colocalizes with ERp57 (F). G: Western blot of nuclear (N) and cytoplasmic (C) fractions from A549 cells. β-tubulin and lamin A/C were used as markers of cytoplasmic and nuclear fractions respectively. These are the results of two independent experiments by duplicate.

80x80mm (300 x 300 DPI)

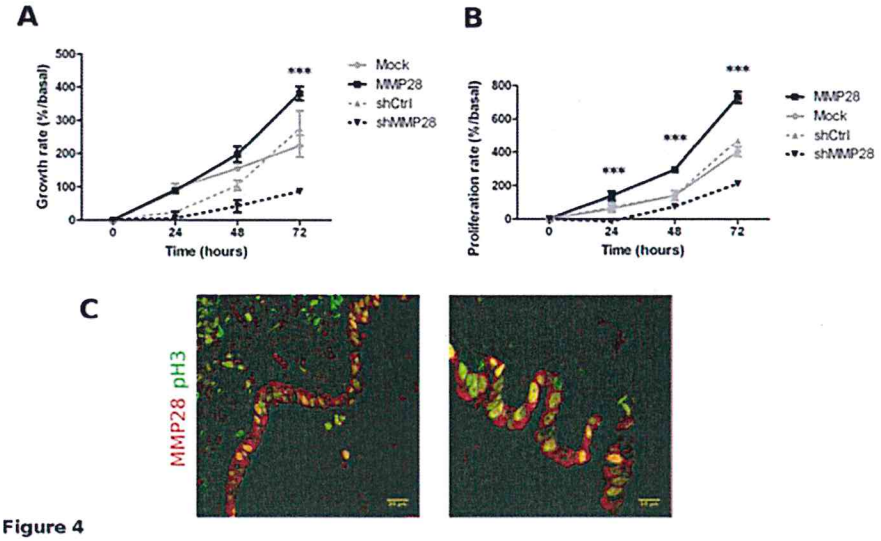

Figure 4

Figure 4. MMP28 induces proliferation in vitro and colocalizes with a proliferation biomarker in IPF lungs. protects from apoptosis and enhances epithelial to mesenchymal transition. MMP28 transfected or silenced A549 alveolar epithelial cells were evaluated for growth rate (A) and proliferation (B). Panels A and B show one representative experiment of four independent experiments by triplicate (data are presented as mean ±SD; ***p<0.001). Panel C show epithelial cells coexpressing anti-phospho-Histone H3, a proliferation marker and MMP28. n=2.

51x33mm (300 x 300 DPI)

AJRCMB Articles in Press. Published on 26-January-2018 as 10.1165/rcmb.2017-0223OC

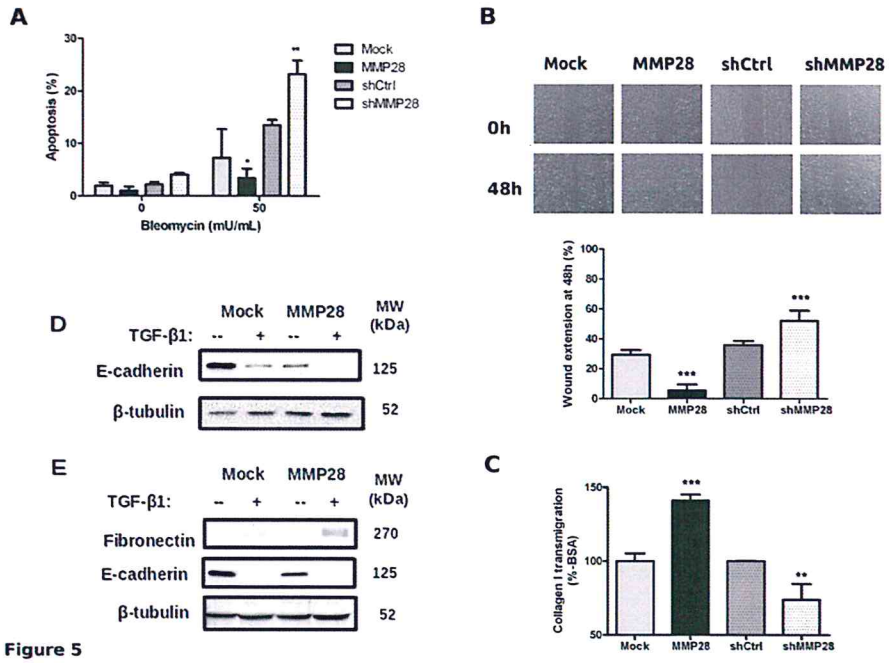

Figure 5. MMP28 protects from apoptosis, promotes migration and enhances epithelial to mesenchymal transition of A549 epithelial cells.
Panel A illustrates the % of apoptosis induced by bleomycin. Results are expressed as mean ±SEM of three independent experiments (*p<0.05, **p<0.01). Panel B: Scratch assays with MMP28 transfected or silenced A549 cells. The magnification is 10x. The figure shows one representative experiment from four experiments performed by quadruplicate. Panel C: Transmigration over collagen I in Boyden chambers. One representative experiment of two independent experiments by triplicate. Panels D and E: Mock and MMP28 transfected cells were stimulated with TGF-β 1 for 2 days (D) and 4 days (E). E-cadherin was used as a marker of epithelial cells, and fibronectin as a marker of mesenchymal cells. Western blots are representative of three independent experiments.

99x72mm (300 x 300 DPI)

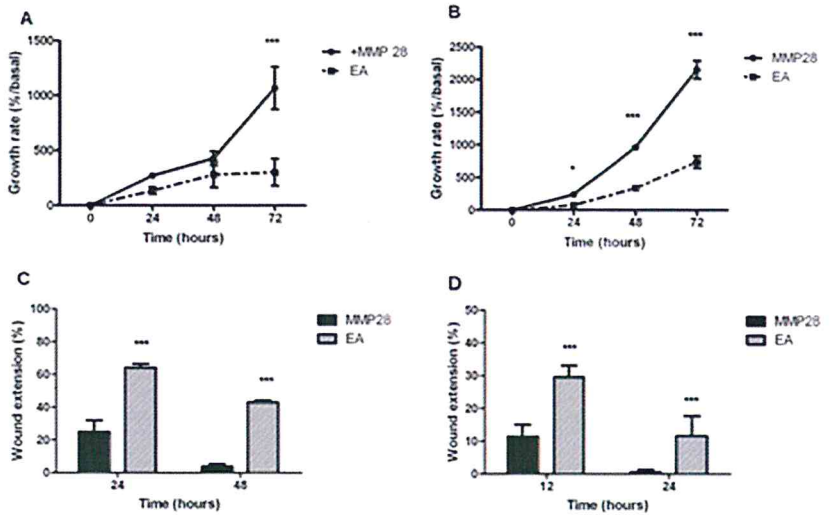

Figure 6

Figure 6. MMP28 effects on migration and proliferation are catalytic-dependent.
Cells were transfected with WT MMP28 (MMP28) or catalytically inactive MMP28 (EA), and proliferation (A and B) and wound closure (C and D) were measured. Each graph is representative of three experiments by triplicate. Data are presented as mean ±SD; *p<0.05, ***p<0.001).

19x15mm (600 x 600 DPI)

AJRCMB Articles in Press. Published on 26-January-2018 as 10.1165/rcmb.2017-0223OC

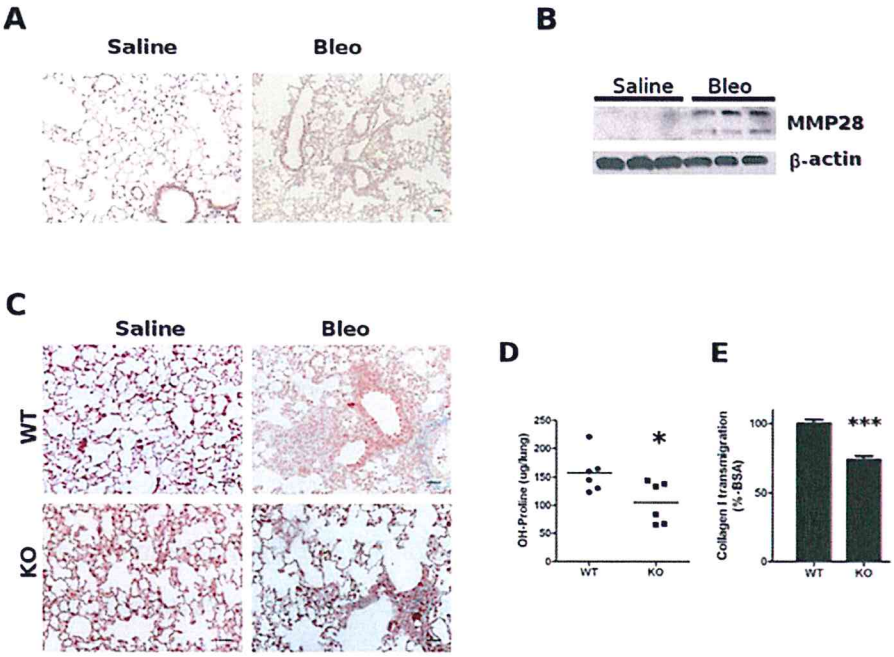

Figure 7

Figure 7. Analysis of Mmp28 in murine pulmonary fibrosis model. WT mice after 14 days of saline or bleomycin instillation: Mmp28 IHC (A), Mmp28 western-blot (B). WT or Mmp28-deficient mice (KO) after 14 days of saline or bleomycin instillation: Masson's trichrome (C), OH-Proline quantification (D), transmigration of lung epithelial enriched fraction over collagen I in Boyden chambers (E). Two independent experiments with n=6.

54x43mm (300 x 300 DPI)

Online Data Supplement

Supplementary Materials and Methods

Bacteria culture and cloning

Cloning experiments were performed with *Escherichia coli* strain XL10-Gold (Agilent). Bacteria cultures were maintained in LB (L1900, Sigma) and LB agar (L2025, Sigma) in an incubator at 37°C. Heat-shock competent bacteria were prepared with $CaCl_2$ 0.1M. Transformed cells were selected with 20μg/mL of kanamicine. Plasmid extraction was performed with the alkaline lysis method and purified with columns (QIAGEN Plasmid Maxi Kit). Plasmid length was measured by electrophoresis after linealization with Xho I (data not shown). MMP28-DDK and empty vector pCMV6-Entry C-terminal Myc and DDK Tagged plasmids were purchased from Origene (RC215325, PS100001). Site-directed mutagenesis (SDM) was performed with QuikChange II XL Site-Directed Mutagenesis Kit (cat.200522, Agilent). Mutagenesis results were corroborated by sequencing with human MMP28 primers and/or plasmid primers (**table E~~1~~2**) at the Molecular Biology Unit in Instituto de Fisiologia Celular, UNAM.

Mammalian cell culture

A549 authenticity was tested by short tandem repeats genetic profile at Instituto Nacional de Medicina Genomica (INMEGEN, Mexico). A549 cells were grown in Ham's F12 (Gibco), with 10% of fetal bovine serum (Gibco). The same media was used for rat AEC supplemented with: 0.01 mg/ml bovine pituitary extract, 0.005 mg/ml insulin, 2.5 ng/ml insulin-like growth factor, 0.00125 mg/ml transferrin, and 2.5 ng/ml epithelial growth factor (EGF). BEC were grown in BEGM (Lonza) with the recommended complements: epinephrin, retinoic acid, bovine pituitary extract, EGF, insulin, hydrocortisone, gentamicin sulfate, amphotericin-B, transferrin and triiodothyronine. BEC were used in passage 4 in

AJRCMB Articles in Press. Published on 26-January-2018 as 10.1165/rcmb.2017-0223OC

all experiments. Differentiated BEC were obtained as explained before (E1), at day 28 the cells were harvested and fixed as citospins for immunofluorescence. Mock and MMP28 transfected cells were stimulated with 5ng/mL of TGFβ1 (Biolegend) in serum-free medium for 2 or 4 days.

Imaging

Immunohistochemistry. Lung tissue sections were deparaffinized, rehydrated, incubated for 30min in H2O2 (3%), followed by heat-induced antigen retrieval with citrate buffer (10mM, pH 6.0) heated in a microwave. Tissue was blocked with Universal Block Solution (BioGenex) for 10min and with sheep serum for 30min, then incubated with the primary antibody solution at 4°C overnight. Incubation with secondary biotinilated antibody was performed at room temperature (RT) for 20 min (BioGenex), followed by incubation with streptavidin-HRP (BioGenex) at RT for 20 min. Finally, signal was developed using 3-amino-9-ethyl-carbazole AEC (BioGenex) in acetate buffer containing 0.05% H_2O_2 as substrate. The sections were counterstained with hematoxylin and mounted with Cristal Mount (Biomeda). Slides were examined under a Nikon microscope with NIS-Elements AR software.

Immunofluorescence. Lung tissue sections were deparaffinized, rehydrated, followed by antigen retrieval with citrate buffer (10mM, pH 6.0) at 125°C 10'' in a decloaking chamber, and then slides were blocked with BSA 4% in PBS 1h. Incubation with primary antibody was performed overnight 4°C, followed by incubation with secondary antibodies for 1h at RT. Cells were fixed with p-formaldehyde 4%, permeabilized with Triton x-100 0.1%, blocked with BSA 4% in PBS, incubated with primary antibody overnight at 4°C, followed by incubation with secondary antibody for 1h at RT, washed and stained with DAPI, mounted with Fluoro Care Anti-Fade Mountant Mounting medium (FP001 G5, G10, Biocare medical), or with Fluorescence Mounting Medium (Dako S30223). Slides were examined under an Axio Imager Microscope (Carl Zeiss) or under a confocal laser-scanning microscope (Olympus FluoView™ FV1000).

Imaging flow cytometry. A549 transfected cells (Mock, WT-MMP28 or KQ-MMP28) were harvested, counted, prepared as 20 million/mL, washed with PBS, fixed with FOXP3 Fix/Perm Buffer (421401, BioLegend) during 20 min at RT, washed and permeabilised with FOXP3 Perm buffer (421402, BioLegend) overnight at 4°C. Incubation with primary antibody was performed in FOXP3 Perm buffer 90 min at RT. Incubation with AF488 conjugated secondary antibody was performed in PBS with BSA 1% 1h at RT. Cells were washed twice and stained with 7-aminoactinomycin D (7AAD, 559925, Bio Legend). 5000 events defined as single cells were acquired at low speed and high sensitivity with the 60x magnification objective in an amnis ImageStream®X Mark II Imaging Flow Cytometer (Merck). Data were analyzed using the nuclear translocation tool of ImageStream Data Exploration and Analysis Software (IDEAS®, Merck).

Silencing and overexpression

AEC were seeded at 80% confluency; next day, lentiviral particles (Santa Cruz) with scrambled control shRNA (sc-108080) or shMMP28 (sc-62278-V) were added with 5ug/mL of polybrene (sc-134220, Santa Cruz) and incubated for 24h. Cells were washed, divided and selected with puromicine for stable transfection. For HBEC silencing, scrambled siRNA (AM4611, Ambion) or siMMP28 (s35627, Ambion) was added to cells with Lipofectamine RNAiMAX (13778-150, Invitrogen), at the time of seeding (reverse transfection). For overexpression, human or rat AEC were seeded at 80% confluency; next day, 1µg of plasmid (MMP28, KQ-MMP28, EA or Mock: RC215325 and pCMV6-Entry C-terminal Myc and DDK Tagged, PS100001 Origene) was added with Turbofectin (TF81001, Origene); after 48h, cells were washed, divided and selected with G418 for stable transfection.

Quantitative PCR. MMP28 expression was analyzed in silenced, transfected and stimulated cells by quantitative polymerase chain reaction (qPCR). Total RNA was isolated using Trizol Reagent (Life Technologies), then cDNA was synthesized with the Verso cDNA synthesis Kit (AB-1453/B, Thermo Scientific), and qPCR was performed with Master Mix

AJRCMB Articles in Press. Published on 26-January-2018 as 10.1165/rcmb.2017-0223OC

(Applied Biosystems) and Taqman probes: hMMP28 and hypoxanthine-guanine phosphoribosyltransferase (HPRT) (Applied Biosystems) as endogenous.

Protein expression. Cells were lysed with RIPA buffer (PBS with IGEPAL 1%, Deoxycholate 0.5% and SDS 0.1%), or fractions were obtained as cytoplasmic and nuclear proteins with the NE-PER kit (78835, Thermo Scientific). Conditioned media were dialyzed with PMSF 0.1 M and NEM 2M (serine and cisteine protease inhibitors), lyophilized and resuspended in 1/100 the initial volume. Proteins were quantified with Bradford (BioRad) or with bicinchoninic acid (BCA) assay (Thermo). Samples for western blot were prepared with sample Laemmli buffer with 2-mercaptoethanol, and heated for 5min at 95°C. SDS-PAGE was followed by humid transfer to nitrocellulose or PVDF membranes, which were blocked 1h at RT with 5% fat-free milk in TBS with 0.05% tween-20 (TBS-T). After overnight incubation with primary antibody at 4°C, membranes were washed with TBS-T, followed by incubation with secondary antibody for 1h at RT, washed again and developed with enhanced chemiluminescence (ECL) system (Thermo Fisher Scientific), detected with ChemiDoc XRS imaging system (Bio-Rad) and analyzed with Image Lab 5.2.1 software (Bio-Rad), including densitometric analysis.

Functional Effects

Growth rate was studied with the WST-1 reagent (Roche). Cells were seeded on 96-well plates, with AEC being seeded at low confluence (~60%) and BEC at medium confluence (~80%). AEC assays were performed in the presence of 1% FBS. Cells were incubated at day zero, one, two and three with serum-free medium and WST-1 reagent for 1h at 37°C (for AEC 5uL of reagent was added to 100uL of medium; while BEC used 10uL of reagent in 100uL of medium). Optic density (OD) was measured at 450 nm and 620 nm as reference. Growth rate was calculated as percent over basal measure (day zero). Three independent experiments per cell type per triplicate were performed.

Proliferation rate was measured with CyQUANT reagent (Thermo Fischer Scientific). Cells were seeded on 96-well plates just as for the growth rate experiments. AEC assay was performed in presence of 1% FBS. Every 24h medium was removed, cells were washed with PBS and wells were frozen at -80°C. At the end, all wells were thawed to RT, and incubated with lysis buffer and CyQUANT GR. Fluorescence was read at 480nm and 520 nm as reference. Proliferation rate was calculated as percent over basal measure (day zero). At least two independent experiments per cell type per triplicate were performed.

Apoptosis. Cells were seeded at 75% confluence and stimulated with 50mU/mL of bleomycin (Bleolem) in serum-free medium for 48h. Cells were harvested and stained with PE Annexin V (556421 BD Biosciences) and 7-aminoactinomycin D (7AAD, 559925, Biolegend). Cells were analyzed by flow citometry in a CANTO flow citometer (BD Biosciences). Results were analyzed with FlowJo software (Tree Star, Inc). Three independent experiments were performed per duplicate.

Wound assay was performed as follows. Cells were seeded at 100% confluence, AEC in six-well plates, rat AEC in 12-well plates, and BEC in 24-well plates. A *scratch* was drawn with a 200uL tip. Images were taken with an inverted EVOS XL microscope (Life Technologies) and analyzed with ImageJ software. Three independent experiments per quadruplicate were performed.

Transwell cell migration. Cells were seeded on Collagen I coated 8µm transwells (QCM Haptotaxis Cell Migration Assay – Collagen1, Colorimetric ECM582 Millipore). 50ng/mL of EGF was used as chemoatractant. After 18h, transwells were stained with crystal violet to measured migration. Cells on BSA-coated chambers were used as blanks for each sample. OD was read at 560 nm. These experiments were performed twice by triplicate.

AJRCMB Articles in Press. Published on 26-January-2018 as 10.1165/rcmb.2017-0223OC

Hydroxyproline quantification

Lungs were hydrolyzed in 1 ml of 6N HCl for 18h at 95°C. Aliquots were measured in a microplate with chloramine T and Ehrlich solution as explained elsewhere (E4). Absorbance was measured at 550 nm, data were expressed as micrograms of hydroxyproline per lung as determined by a standard curve.

In silico motives search. MMP28 sequence was evaluated by two different free software tools: *PredictProtein* (E2) and *NLStradamus* (E3), prediction cutoff 0.7.

Lung epithelial enriched cell fraction.

Lung epithelial enriched cell fraction. Mice lung epithelial cells were isolated by negative selection. Enzymatic digestion of the lungs was performed, cell suspension was incubated with erythrocyte lysis buffer, and negative selection was performed with CD45 beads. The filtered cell suspension had 85% purity of epithelial cells verified by flow cytometry.

Antibodies.

From abcam: ERp57 ab13506, cytokeratin 5 (CK5) ab52635, fibronectin [IST-2] ab6435. From Sigma-Aldrich β-actin (ACTB) HRP-conjugated anti-ACTB. From Cell signaling lamin A/C (2032). From Biogenex E-cadherin AM390-10M. From Biolegend β-actin 622101. From Santa Cruz: pan-cytokeratin sc8018, proSPC sc-293169 and Mmp28 sc-367259 (figure E6). From EMD Millipore 05-806 Anti-phospho-Histone H3 (Ser10) Antibody, clone 3H10. From Life Technologies fluorescent secondary antibodies and reagents: goat anti-rabbit AF568 A11011; donkey anti-mouse AF488 A11001; DAPI: NucBlue R37606. From Novus Biologicals: MMP28 NBP2-17314 (figure 2, 3A-C). From Origene: DDK, TA50011-100 and TA180144. From Amersham: anti-mouse and anti-rabbit. From Triple Point Biologics: RP2-MMP28 (figure 2, E1), RP3-MMP28 (figure 2, E2), RP4-MMP28 (figures 2, 3E-G, 4, E1, E2), SPA-MMP28 (figure 1, 2, 3A-D, E2). RP2-MMP28 binds to the prohormone convertase

region (beginning of the catalytic domain), RP3-MMP28 binds to the hinge domain, RP4-MMP28 binds to the hemopexin-like domain; SPA-MMP28 is a pool that contains RP2, RP3 and RP4-MMP28.

Table E1.

Demographic characteristics of the patients included in the study

Patients	Mexico	Germany
n	17	9
Gender (M:F)	14:3	7:2
Age (years)	61.7 ± 7.5	56.1 ± 8.6

Table E2.

Oligonucleotides used for plasmid sequencing and site-directed mutagenesis (SDM).

Primer	Forward (5' - 3')	Reverse (5' - 3')
MMP28	CAGCTGGGACGACGTGCTGG	GCGTTTCAGGGCGCCTTCCT
Plasmid	GGACTTTCCAAAATGTCG	ATTAGGACAAGGCTGGTGGG
EA SDM	GCTGGCGCACGCGATCGGTCACACG CTTGGCC	GGCCAAGCGTGTGACCGATCGCGTGCGCC AGC
KQ SDM	GACACCGGACCCAAATGAGGCGTCA GCAACGCTTTGC	GCAAAGCGTTGCTGACGCCTCATTTGGGTC CGGTGTC

AJRCMB Articles in Press. Published on 26-January-2018 as 10.1165/rcmb.2017-0223OC

Supplementary references

(E1) Schamberger AC, Staab-Weijnitz CA, Mise-Racek N, Eickelberg O. Cigarette smoke alters primary human bronchial epithelial cell differentiation at the air-liquid interface. *Sci Rep*. 2015;5:8163.

(E2) Rost B., Yachdav G., Liu J. ThePredictProtein Server. Nucleic Acids Research 2004;32(Web Server issue):W321-W326 http://www.predictprotein.org

(E3) Nguyen Ba AN, Pogoutse A, Provart N, Moses AM. NLStradamus: a simple Hidden Markov Model for nuclear localization signal prediction. BMC Bioinformatics. 2009;10(1): 202 http://www.moseslab.csb.utoronto.ca /NLStradamus/

(E4) Cabrera S, Maciel M, Herrara I, Nava T, Vergara F, Gaxiola M, López-Otín C, Selman M, Pardo A. Essential role for the ATG4B protease and autophagy in bleomycin-induced pulmonary fibrosis. Autophagy. 2015; 11(4):670-84.

Supplementary Figures Legends

Figure E1. ***Confocal images revealed nuclear staining of MMP28 in alveolar epithelial cells.*** Z-stacking in IPF tissue with apparent nuclear MMP28 was analyzed. Orthogonal views at three different cells in this area shows that the signal in some cells was inside the nucleus (A, B), and in others was perinuclear (C). Panels D and E show pancytokeratin and keratin 5 (krt5) expression in A549 cells. Panel F: negative control. N=2.

Figure E2. ***Mutation of lysines in probable NLS does not affect nuclear localization of MMP28.*** **Pannel A:** Graphics show the percentage of cells with colocalization of MMP28 or tag and DNA. The figure represents the mean of two independent experiments ±SEM where 5000 events defined as single cells were acquired at low speed and high sensitivity with the 60x magnification objective. **B:** Representative images of cells obtained by confocal flow cytometry (via ImageStream, see supplementary methods) showing localization of transfected DDK-tagged wildtype MMP28 (WT-MMP28) or mutant MMP28 (KQ-MMP28). Transfected proteins were detected with anti-DDK (tag) antibody (green). DNA was stained with 7AAD (red).

Figure E3. ***Overexpression and silencing of MMP28 in vitro***. A and B: qPCR and Western blot of A549 transfected cells. C and D: qPCR and Western blot of A549 silenced cells. E and F: qPCR and Western blot of rat AEC transfected with human MMP28. G and H: Transient silencing of bronchial epithelial cells with scrambled (scr) or siMMP28 (si28). DDK: tag marker. CM: conditioned media.

Figure E4. ***MMP28 increases growth rate of rat alveolar epithelial cells and human bronchial epithelial cells.*** (A, B): Growth and proliferation rates of rat AEC transfected with human MMP28. (C, D): Growth and proliferation rates of MMP28 silenced BEC. Each

AJRCMB Articles in Press. Published on 26-January-2018 as 10.1165/rcmb.2017-0223OC

graph is representative of at least two experiments by triplicate. Data are expressed as mean ±SD, (**p<0.01, ***p<0.001).

Figure E5. ***MMP28 promotes wound closure of rat alveolar epithelial cells and human bronchial epithelial cells.*** Scratch assays with transfected rat AEC (A) and silenced BEC (B). Graphs are representative of three experiments by quadruplicate. Data are presented as mean ±SD (*p<0.05, ***p<0.001).

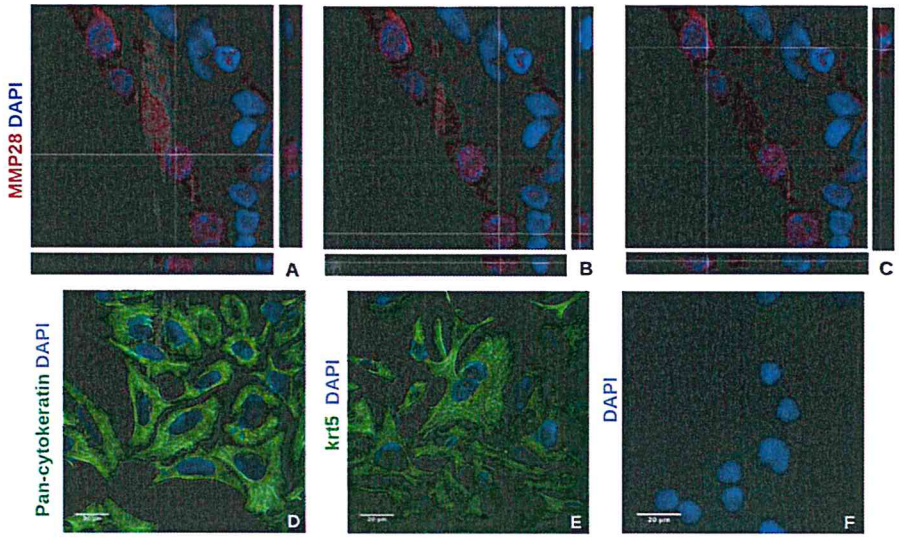

Figure E1

Figure E1. Confocal images revealed nuclear staining of MMP28 in alveolar epithelial cells. Z-stacking in IPF tissue with apparent nuclear MMP28 was analyzed. Orthogonal views at three different cells in this area shows that the signal in some cells was inside the nucleus (A, B), and in others was perinuclear (C). Panels D and E show pancytokeratin and keratin 5 (krt5) expression in A549 cells. Panel F: negative control. N=2.

155x109mm (300 x 300 DPI)

AJRCMB Articles in Press. Published on 26-January-2018 as 10.1165/rcmb.2017-0223OC

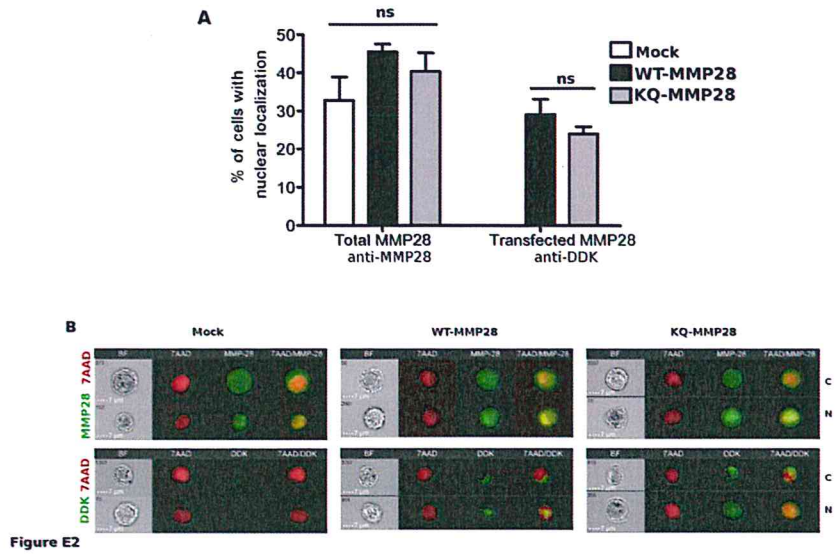

Figure E2. Mutation of lysines in probable NLS does not affect nuclear localization of MMP28. Pannel A: Graphics show the percentage of cells with colocalization of MMP28 or tag and DNA. The figure represents the mean of two independent experiments ±SEM where 5000 events defined as single cells were acquired at low speed and high sensitivity with the 60x magnification objective. B: Representative images of cells obtained by confocal flow cytometry (via ImageStream, see supplementary methods) showing localization of transfected DDK-tagged wildtype MMP28 (WT-MMP28) or mutant MMP28 (KQ-MMP28). Transfected proteins were detected with anti-DDK (tag) antibody (green). DNA was stained with 7AAD (red).

109x75mm (300 x 300 DPI)

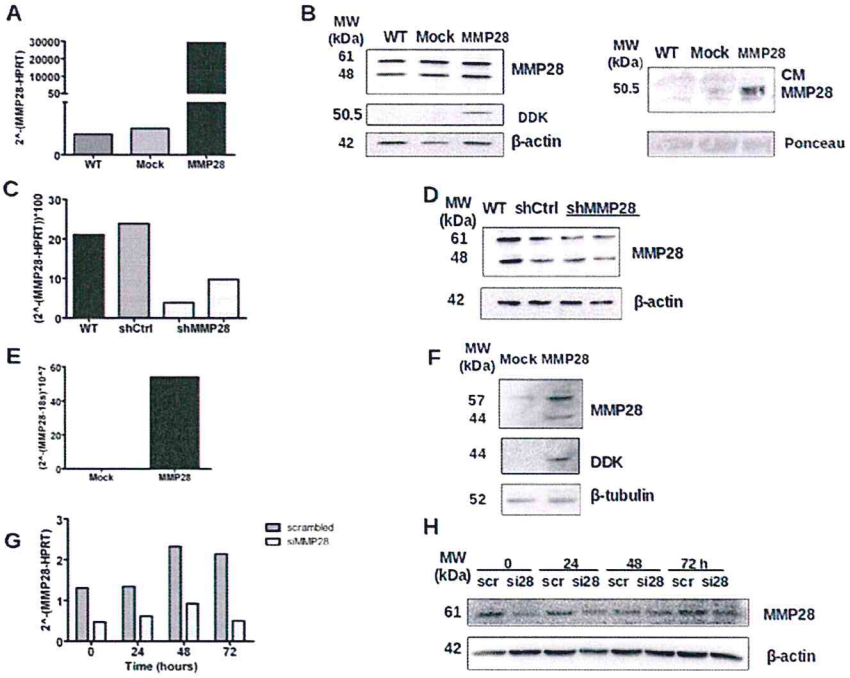

Figure E3

Figure E3. Overexpression and silencing of MMP28 in vitro. A and B: qPCR and Western blot of A549 transfected cells. C and D: qPCR and Western blot of A549 silenced cells. E and F: qPCR and Western blot of rat AEC transfected with human MMP28. G and H: Transient silencing of bronchial epithelial cells with scrambled (scr) or siMMP28 (si28). DDK: tag marker. CM: conditioned media.

80x80mm (600 x 600 DPI)

AJRCMB Articles in Press. Published on 26-January-2018 as 10.1165/rcmb.2017-0223OC

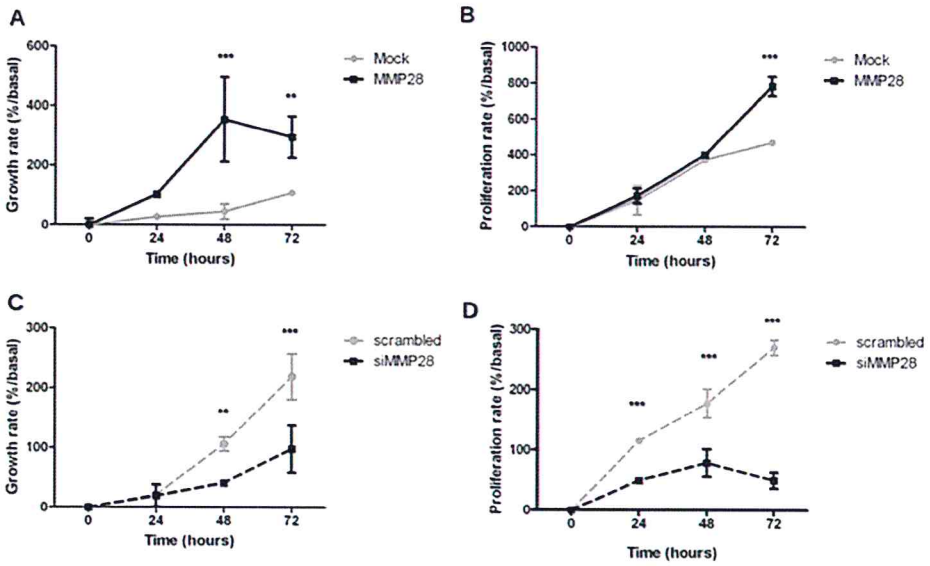

Figure E4

Figure E4. MMP28 increases growth rate of rat alveolar epithelial cells and human bronchial epithelial cells. (A, B): Growth and proliferation rates of rat AEC transfected with human MMP28. (C, D): Growth and proliferation rates of MMP28 silenced BEC. Each graph is representative of at least two experiments by triplicate. Data are expressed as mean ±SD, (**p<0.01, ***p<0.001).

28x19mm (600 x 600 DPI)

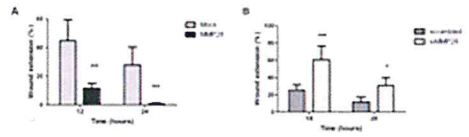

Figure E5

Figure E5. MMP28 promotes wound closure of rat alveolar epithelial cells and human bronchial epithelial cells. Scratch assays with transfected rat AEC (A) and silenced BEC (B). Graphs are representative of three experiments by quadruplicate. Data are presented as mean ±SD (*p<0.05, ***p<0.001).

11x4mm (600 x 600 DPI)